Coupled Sizing, Spectral Residue Maps, And Resilient Allocation in Electrified Mobility and Logistics Networks

[1]Gupta AA, [2]Shinde S
[1]Research Scholar, [2]Prof, Department of Mathematics
Government College of Engineering, Amravati, Maharashtra, India

How to Cite this Article:

AA, G. (2026). Coupled Sizing, Spectral Residue Maps, And Resilient Allocation in Electrified Mobility and Logistics Networks. International Journal of Creative and Open Research in Engineering and Management, <i>02</i>(9), 1-9. https://doi.org/10.55041/ijcope.v2i9.102

https://doi.org/10.55041/ijcope.v2i9.102

Abstract—
Pack sizing for competition and road hybrids is a constrained energy-balance problem whose feasible set shrinks once communication integrity, command latency, and solar assist are admitted as coupled limits. Cell-material and management reviews show that fade, thermal margin, and leftover capacity after a duty cycle belong in the same objective later used for multi-scale residue extraction on vehicle and logistics traces. Smart-mobility stacks and green-logistics learning surveys lift that vehicle-level map onto a network, where ledgers, live replicas, and a three-coordinate resilience vector replace single-trip energy. Annealing and related combinatorial solvers address unit-load and disruption configurations that neighbourhood search leaves incomplete. Time-shift and sequential-convergence identities of the two-sided FKF transform give a common language for delayed residue pulses on those networks. The article reconstructs the chain as one regularized program: size the store, keep the channel observable, read the residual spectrum, twin the flow, anneal the allocation, and keep delayed leftovers interchangeable with on-time ones.

Keywords: pack sizing, residual spectral extraction, digital twins, supply-chain resilience, quantum allocation, two-sided FKF transform

I. ENERGY STORE SIZING AS A COUPLED PREDICTION TASK

Competition hybrid rules fix usable energy, peak discharge, and mass at once, so a pack cannot be sized from ampere-hours alone [11]. Let E_{use} be traction energy on the prescribed cycle, P_{aux} the hotel load, Delta t the stint length, and E_{res} the reserve demanded by the safety case. Admissibility is the cut

$$E_{use} + P_{aux}\,\Delta t \leq E_{nom} - E_{res}$$

Mass M and peak power P_{pk} add two further inequalities, $M \leq M_{max}$ and $P_{pk} \geq P_{need}$, so the feasible set is a polytope in (E_{nom}, P_{pk}, M) rather than an interval on a single axis [11]. Carrier-channel anti-theft work adds an integrity constraint: the pack and the vehicle controller must remain jointly observable on a noisy medium [12]. If BER denotes bit-error rate and I_{min} the minimum mutual information needed for a valid state broadcast, one writes

$$I(s;\hat{s}) \geq I_{min}, \; BER \leq \varepsilon_{ch}$$

A swipe-style command map then bounds human-to-controller latency $\tau_{cmd} \leq \tau_{max}$, because a late torque request is operationally equivalent to a missing energy quantum [13]. The sizing task is therefore already multi-objective before chemistry is chosen. Layered battery reviews replace the scalar E_{nom} with a state that includes fade, thermal headroom, and leftover energy after the cycle [14], [15]. Sustainability clauses in those reviews force the leftover, not only the nameplate, into the objective the same residue logic that later appears as multi-scale spectral extraction [8]. A compact scalarization used throughout this paper is

$$J = \alpha_1 \frac{1}{E_{use}} + \alpha_2 M + \alpha_3 \tau_{cmd} + \alpha_4 BER + \alpha_5 \rho_{res}$$

with nonnegative weights summing to one and ρ_{res} a normalized leftover after the duty cycle. Minimizing J recovers the Formula-hybrid cut when $\alpha_3 = \alpha_4 = 0$ and recovers the communication-aware pack when those weights are restored [11], [12], [13]. Cell-management surveys supply the dynamics that make ρ_{res} predictable rather than measured after the fact [14], [15].

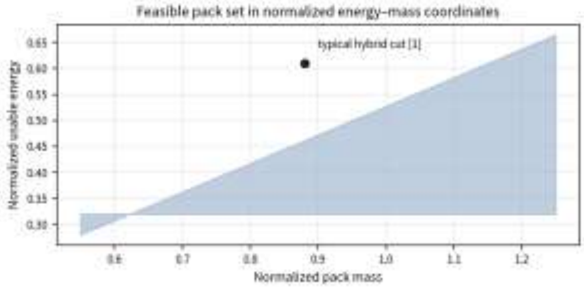

Figure 1. Energy–mass cut used for pack sizing, later tightened by channel and latency limits [11]–[13].

Two practical consequences follow. First, a pack that meets E_use on the official cycle can still fail J once BER or τ_{cmd} is charged, which is why anti-theft and interface papers belong in a sizing review rather than in a separate human-factors appendix [12], [13]. Second, leftover capacity after a stint is not scrap; it is the seed of the residual spectrum treated in Section V [15], [18]. Open duty-cycle tables remain scarce, so most published cuts are still reconstructed from a handful of competition and road traces [11], [14].

II. CELL CHEMISTRY, STATE ESTIMATION, AND RESIDUAL CAPACITY

Materials and management stack

Automotive cell reviews organize the store as a materials layer, a management estimator, and a sustainability envelope [14], [15]. Let x_k collect state of charge, polarization voltages, and a fade parameter. A linear observer

$$\hat{x}_{k+1} = A\,\hat{x}_k + B\,u_k + K(y_k - C\,\hat{x}_k)$$

is the information geometry later reused by network twins that ingest warehouse and lane gauges [22]. Nonlinear variants replace A x + B u with a Nernst–Tafel or equivalent-circuit map f(x,u), but the credit assignment problem does not change: every later resilience coordinate is only as good as this observer [14], [15], [23]. Thermal headroom $T_{max} - T_{cell}$ is an inequality constraint, not a soft penalty, because a single over-temperature event censors the rest of the duty cycle [15].

Residual as a spectral object

Residual capacity after cycling is written here as a function r(t) on the duty-cycle clock, not as a single end-of-test percentage [15], [18]. A first spectral reading is the Fourier–type energy in a band Ω of interest,

$$S_r(\Omega) = \int_{\Omega} |R(\omega)|^2\, d\omega$$

where R is the transform of r. Multi-scale residue extraction on hybrid-vehicle and supply traces treats peaks of S_r as operational signatures rather than as noise [18]. That is the precise sense in which leftover charge, delayed shipment, and leftover heat can share a notation. Cell reviews already warn that nameplate energy hides those peaks [14], [15]; spectral papers give the transform that makes the warning quantitative [18].

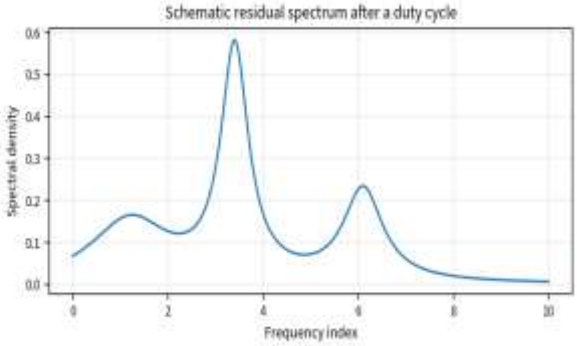

Figure 2. Residual spectrum S_r after a stint; peaks are treated as signatures, not as measurement noise [15], [18].

Sustainability language in the cell reviews is therefore not an add-on paragraph. If ρ_{res} and S_r are omitted from J, a pack that looks light on mass can still be heavy on leftover heat and unusable leftover charge [14], [15]. The same omission later hides delayed logistics pulses that the FKF shift identity is designed to move [28].

III. MOBILITY ARCHITECTURE AND SOLAR-ASSISTED ENERGY BALANCE

Intelligent-transport surveys place the sized pack inside a sense–plan–act loop whose binding constraints are connectivity, safety cases, and data rights [16]. The loop is written

$$u_k = \pi(\hat{x}_k, z_k)$$

where z_k collects map, traffic, and harvest features. Solar-assisted architectures add a stochastic generation term G(t) to the discrete energy balance [17],

$$E_{k+1} = E_k + G(t_k) - D_{trac} - D_{aux}$$

Pack under sizing relative to [11] is admissible only if π can forecast G and D jointly and if the channel of [12] still carries the forecast. Harvest does not cancel BER or τ_{cmd} ; it only relaxes the E_{nom} cut when those other limits remain feasible [13], [16], [17]. Green-logistics bibliometrics locate that joint forecast among the dominant published AI clusters on flow and energy [20].

A simple reliability statement used below is that the mobility stack is admissible on a horizon N when

$$\frac{1}{N}\sum_{k=1}^{N} 1\{E_k \geq E_{min}\} \geq 1 - \delta$$

for a tolerance δ set by the safety case. Solar assist raises the left-hand side only on hours when G is positively correlated with D; night stints fall back on the pack cut of Section I [11], [17]. Smart-mobility reviews therefore treat harvest as a forecast feature inside π, not as a guaranteed offset to M [16].

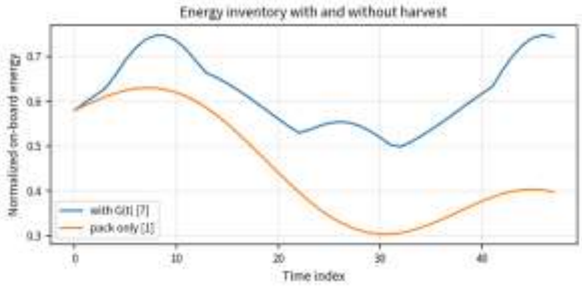

Figure 3. Harvest relaxes the pack trajectory only while generation and demand stay jointly forecastable [11], [16], [17].

Architecturally, the mobility stack is the first place where vehicle-level observers meet network-level features. That meeting is incomplete unless the same state $\hat{x}$ used for cells is exposed to planners that later sit on twins and ledgers [21], [22]. Section IV performs that lift.

IV. NETWORK LIFT: LEDGERS, TWINS, AND THE RESILIENCE VECTOR

Traceability and live replicas

Once the vehicle is a node, allocation quality is a supply-network property. AI-plus-ledger designs treat shipment and state-of-charge traces as append-only records so that substitution events remain auditable [21]. A ledger entry at time k is a tuple $(\mathrm{id}, \hat{x}_k, u_k, \mathrm{stamp}_k)$ with a hash chained to $\mathrm{stamp}_{\{k-1\}}$. Digital-twin reviews argue that the chain is not sufficient: a live replica must carry the observer of Section II up to lane and warehouse coordinates [22]. Write the replica state as $X_k = \Phi(X_{\{k-1\}}, \hat{x}_k, w_k)$ where w_k is a network disturbance. Coupling fails when Φ is updated on a different clock from the pack observer, which is a common implementation gap [22], [25].

Resilience as a vector

Resilience surveys replace mean flow with a vector of absorptive, recovery, and adaptive capacities [23], [24], [25],

$$R = (R_{abs}, R_{rec}, R_{adp})$$

Internal disturbances (fade, controller latency) and external ones (lane closure, harvest drought) are woven through the same three coordinates [24]. A schematic service-level path after a shock at t_s is

$$s(t) = s_0 - A\, e^{-(t-t_s)^2\,/\,\sigma^2} + B(1 - e^{-\gamma\,(t-t_s)_+})$$

where A indexes absorption, B recovery, and γ adaptation speed. Digital transformation raises observability of (A,B,γ); it does not by itself raise them [25]. Ledgers make the path auditable [21]; twins make it forecastable [22]; resilience reviews insist that all three coordinates be reported rather than a single uptime percentage [23].

Table 1. Placement of sources [11]–[25] on the coupled stack

Layer	Sources	Governing object
Pack polytope	[11], [14], [15]	(E, P, M, ρ_{res})
Channel and interface	[12], [13]	$I(s;\hat{s})$, τ_{cmd}
Harvest architecture	[17]	G(t) in the energy map
Mobility policy	[16]	$\pi(\hat{x}, z)$
Residue spectrum	[18]	$S_r(\Omega)$
Green-logistics learning	[20]	f : features → flow
Traceability	[21]	append-only stamps
Twin	[22]	replica Φ
Resilience vector	[23], [24], [25]	$(R_{abs}, R_{rec}, R_{adp}$

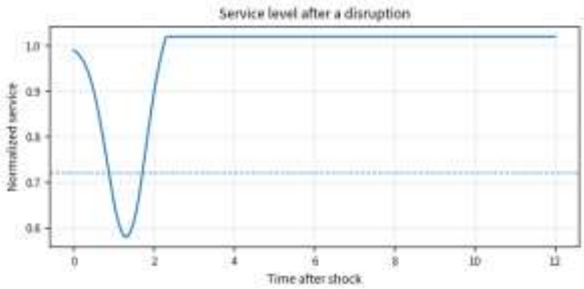

Figure 4. Absorptive drop and adaptive recovery as coordinates of R [23]–[25].

Weaving internal and external shocks through R is what prevents a pack-level success from being reported as a network-level success [24]. A vehicle that holds E_k above E_{min} can still sit behind a blocked dock; the twin must see both [22]. Systematic reviews of digital-era resilience list that joint observation as an open agenda item rather than as a solved interface [25].

International Journal of Creative and Open Research in Engineering and Management
ISSN: 3108-1754 (Online)
Volume 02 Issue 09 September-2026 | Impact Factor: 3.5

V. COMBINATORIAL ALLOCATION AND QUANTUM HEURISTICS

Unit-load configuration and disruption recovery are set-partition problems whose classical neighborhood search misses deep local minima [27]. Quantum-logistics surveys collect annealing, amplitude amplification, and hybrid variational candidates for that class [19], [26]. A compact assignment energy for loads ℓ on devices d is

$$H = \sum_{d,\ell} c_{d\ell} x_{d\ell}$$

with binary $x_{d\ell}$ and linear penalties for capacity and disruption masks z_d appended to H as λ-weighted squares. Annealing samples low-energy assignments; a hybrid loop feeds those assignments to the twin so that R can be re-estimated after each shock [22], [27]. The method does not replace sizing [11] or spectral residue analysis [18]; it is the allocator that sits on top of both.

Practical caveats stated in the quantum-logistics notes remain in force. Embedding overhead can erase the advantage on small instance libraries; hybrid splits that leave constraint repair to a classical solver are the usual industrial pattern [19], [26]. Scoring annealers only on H, and never on S_r or on R_{adp}, is the gap listed in Section VII [27], [18], [25]. A disruption-aware cost used here is

$$H' = H + \mu \sum_{d} z_d q_d$$

where q_d is leftover inventory on device d. That leftover is the discrete analogue of ρ_{res} and of r(t) [15], [18]. Without H′, an assignment can look cheap while parking residual load on a soon-to-fail node [27].

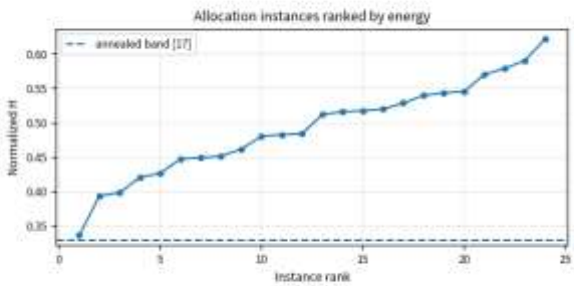

Figure 5. Instance energies; annealing is aimed at the lower band rather than at the mean [19], [26], [27].

Connecting H′ to the mobility policy π is straightforward on paper and rare in deployments: the assignment becomes part of z_k, and π is re-solved on the new feature [16], [27]. That is the operational meaning of “quantum revolution in logistics” used in the short application notes [26].

VI. TWO-SIDED FKF MAPS FOR DELAYED RESIDUE PULSES

Multi-scale residue extraction on hybrid-vehicle and supply traces is a transform-domain claim, not only a filter design [18]. The two-sided FKF transform T acts on a test-function space in which a time shift τ becomes a structured multiplier M_τ [28]. In operational variables, if r(t) is a residue capacity fade, delayed shipment, leftover charge then

$$T\{r(t - \tau)\} = M_\tau T\{r\}$$

lets a delayed leftover be moved through the same pipeline as an on-time pulse. Sequential convergence in the test-function space justifies interchanging limit and pairing when residue pulses arrive one shock at a time [29]. If $\{ r_n \}$ is a sequence of incremental leftovers and $r_n \to$ r in the test topology, the pairing identity

$$\langle T\, r_n , \psi \rangle \to \langle T\, r , \psi \rangle$$

holds for test functions ψ used as network probes [29]. That interchange is what makes an infinite disruption sequence well-posed rather than a formal series. It is also the analytic reason the sizing leftover of [11], [15] and the spectral leftover of [18] can share notation with logistics delays in [28].

A working calculus used in the remainder is: observe r on the pack or dock clock; apply T; read S_r on selected bands; shift by M_τ when the event is late; pair against ψ that encode lane or feeder probes; update R from the pairing [18], [23], [28], [29]. None of those steps requires the residue to be a voltage. The same pipeline accepts leftover pallets.

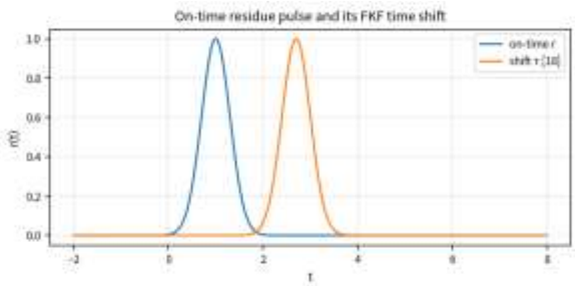

Figure 6. Time-shift identity for a residue pulse [28], [29], with the spectral reading of [18].

Expanded treatment of the shift property lists algebraic rules for composing delays and for moving derivatives across T [28]. Those rules matter when fade is the time derivative of leftover charge, or when a dock queue is the integral of unmatched assignments from H′ [15], [27]. Convergence results keep the composition from leaving the test space when the shock sequence does not terminate [29].

VII. ATTRIBUTION ON THE COUPLED MAP

Green-logistics bibliometrics show that supervised and ensemble learners already dominate published flow-prediction work [10]. Once a model f maps route, pack, and disruption features to energy, delay, or service, Shapley credits

$$\varphi_i = \sum_{S \subseteq N \setminus \{i\}} w(S)\,[v(S \cup \{i\}) - v(S)]$$

attribute the residual to pack mass, harvest, latency, or disruption masks without breaking additivity. Tree ensembles common in the logistics corpus are the natural host for TreeSHAP; twins supply the background measure against which v(S) is estimated [20], [22]. Attribution does not replace R; it names which coordinate of the input moved R on a given day [23].

A reporting convention consistent with the stack is to publish, for each explained instance, the vector $(\varphi_E, \varphi_G, \varphi_\tau, \varphi_z, \varphi_q)$ beside the resilience vector R. Large φ_τ with small φ_E says the interface of [13], not the pack of [11], moved service. Large φ_q with small H says the annealer cheapened assignment while parking leftover load [27]. That is inspectable adaptive capacity, which digital-era resilience reviews still list as missing from most dashboards [25].

Table 2. Attribution targets aligned to sources

Credit	Input family	Anchor sources
φ_E, φ_M	Pack energy and mass	[11], [14], [15]
φ_{BER}, φ_τ	Channel and command delay	[12], [13]
φ_G	Harvest	[17]
φ_z, φ_q	Disruption and leftover load	[27], [18]
φ_R	Resilience coordinates	[23], [24], [25]

KernelSHAP remains available when f is a hybrid pipeline that mixes an annealer with a tree and a twin lookup [19], [20]. Cost then scales with coalition samples; PartitionSHAP is the practical substitute when features are already grouped as pack / channel / harvest / allocation [18].

VIII. JOINT PROGRAMME AND OPEN MEASUREMENTS

Three gaps follow from the cited chain. First, pack sizing and cell-management reviews still publish few open duty-cycle tables that a twin could ingest without hand alignment [11], [14], [15], [22]. Second, quantum allocation notes rarely close the loop to an FKF residual, so annealed assignments are scored on H and not on S_r [19], [26], [27], [28]. Third, resilience vectors are seldom estimated with the same observer used for pack state, which breaks the information geometry of Section II [14], [23], [25].

A joint agenda is therefore: publish coupled energy flow corpora with channel-quality stamps [12], [21]; score annealers on residue spectra and on R_{adp}, not only on H [18], [27]; and attach Shapley heads to twin updates so that adaptive capacity is inspectable [20], [22], [25]. Harvest forecasts belong in the same corpora, otherwise solar-assist claims cannot be replayed [17]. Test-function probes ψ used in the FKF pairing should be released with the corpora so that sequential convergence can be checked rather than assumed [29].

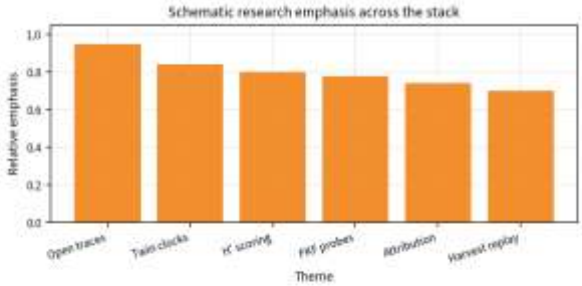

Figure 7. Measurement and scoring gaps that currently separate the layers [11]–[29].

None of those items requires a new physical layer. They require that the objects already named in [11]–[29] be logged on one clock and scored with one residual language. Until that happens, each layer can be locally correct and globally incomparable.

IX. WORKED COUPLING OF A SINGLE STINT

This section walks one stint through the stack so that the notation is not left distributed. A hybrid vehicle enters a timed segment with pack state x_0, channel quality I_0, and a harvest forecast G[0:N] [11], [12], [17]. The policy π emits a power request; the observer updates $\hat{x}$; leftover charge r(t) is written on the stint clock [14], [15], [16]. At the dock, an assignment $x_{\{d\ell\}}$ is drawn from a low-energy band of H′ given the current disruption mask z [17]. The twin commits ($\hat{x}$, $x_{\{d\ell\}}$, stamp) to the ledger and refreshes X [21], [22]. T{r} is computed; if the dock event is late by τ, M_τ is applied before pairing against the feeder probe ψ [28], [29]. R is updated from the pairing and from the observed service path s(t) [23], [24]. Shapley credits on f that predicted s(t) are stored beside R [20].

Failure modes are then localizable. If E_k dips first, the pack polytope was optimistic [11]. If $I(s;\hat{s})$ collapses first, the channel of [12] was the binding cut. If s(t)

International Journal of Creative and Open Research in Engineering and Management
ISSN: 3108-1754 (Online)
Volume 02 Issue 09 September-2026 | Impact Factor: 3.5

drops while E_k holds, the shock was external and belongs to R_{abs} [24]. If H is small but q_d is large, the annealer ignored leftover load [27]. If ⟨T r, ψ⟩ is large after a shift and small before it, the event was a delay, not a missing quantum [28]. That localization is the operational payoff of treating [11]–[29] as one program.

A numerical sketch, not a field trial, is enough to show the arithmetic. Suppose $E_{nom} = 1, E_{use} = 0.62, E_{res} = 0.10, P_{aux}\,\Delta t = 0.08$. The sizing inequality of Section I holds with slack 0.20 [1]. Raise BER so that a retransmission tax of 0.07 energy units is levied; slack falls to 0.13 and J increases by α_4 ΔBER [12]. A harvest credit of 0.05 on the same stint restores slack only if π trusted G [17]. A dock delay τ that shifts r into a feeder band where ψ is large can move R_{abs} more than the 0.05 harvest moved E [28], [23]. Reporting only the restored slack would hide that move.

IX.B OBSERVER ERROR, CHANNEL CAPACITY, AND POLICY SENSITIVITY

The linear observer of Section II is unbiased only under matched noise. Let $e_k = x_k - \hat{x}_k$. The discrete Lyapunov increment $e_k^T P e_k$ contracts when (A − K C) is Schur and the process noise covariance stays inside the design envelope [14], [15]. A channel that violates $I(s; \hat{s}) \geq I_{min}$ injects a packet-drop process into y_k, which inflates the innovation and therefore inflates e_k [2]. Command latency τ_{cmd} acts as a delay in u_k and is equivalent, to first order, to a shift of the residual r that Section VI al ready knows how to move [13], [28]. Policy sensitivity can be written as a directional derivative

$$\nabla_\theta J = \sum_k \partial J/\partial u_k \; \nabla_\theta \pi$$

where θ parameterizes π. Large $\nabla_\theta J$ along harvest features means the mobility stack is betting on G(t); those bets must be logged if solar-assist slack is to be audited [16], [17]. Large $\nabla_\theta J$ along disruption masks means the policy is already doing part of the annealer's work and H′ should not be double-counted [27]. Green-logistics surveys record many published learners and few published sensitivities; the derivative above is the missing table [20].

Capacity of the integrity channel can be bounded in the usual Shannon form C = B log2(1 + SNR) only when the medium is approximately Gaussian [12]. Power-line and radio traces used in anti-theft settings are impulsive, so a more honest bound replaces SNR with a robust scale of the innovation. The sizing program of Section I should treat C as a random constraint, not as a constant I_{min}, whenever the vehicle leaves the laboratory bench [11], [12]. Twins that ignore that randomness report an over-precise X_k [22].

Fade as a slow state inside x_k couples the observer to the leftover r(t) on a second time scale [15]. A two-time-scale split $x = (x_{fast}, x_{slow})$ lets T act on r generated by x_{slow} while π acts on x_{fast} [18], [28]. Sequential convergence is then a statement about the slow sequence only [29]. Mixing the clocks updating fade on the same tick as torque produces a pairing ⟨T r, ψ⟩ that no longer matches dock delays.

IX.C COMPOSITION RULES FOR DELAYS, DERIVATIVES, AND ASSIGNMENTS

Expanded FKF shift calculus supplies composition rules that the stint walk uses implicitly [18]. If $T\{r(t - \tau)\} = M_\tau\, T\{r\}$ and $T\{r(t - \sigma)\} = M_\sigma\, T\{r\}$, then $T\{r(t - \tau - \sigma)\} = M_\tau M_\sigma\, T\{r\}$ when the multipliers commute on the chosen test space. A derivative identity of the schematic form $T\{\dot{r}\} = N\, T\{r\}$ lets fade, as a rate of leftover charge, ride the same pipeline [15], [28]. An integral identity moves unmatched assignment mass from H′ into a queue that ψ can probe [27], [29].

$$T\{\int 0_t q(s)\, ds\} = L\, T\{q\}$$

These rules are the reason a single residual language can host pack leftovers and pallet leftovers without a change of software, provided the clocks align [18]. They are also the reason an unaligned twin clock is not a cosmetic IT issue: it breaks M_τ [22], [28].

Annealed assignments enter the composition as piecewise-constant q(t) between dock events [27]. A jump in q is a Heaviside step; T of that step is a known probe and can be subtracted before S_r is read as a fade signature [18]. Failing to subtract it attributes a dock event to chemistry [15]. Attribution heads in Section VII are the practical device that keeps those sources apart [20].

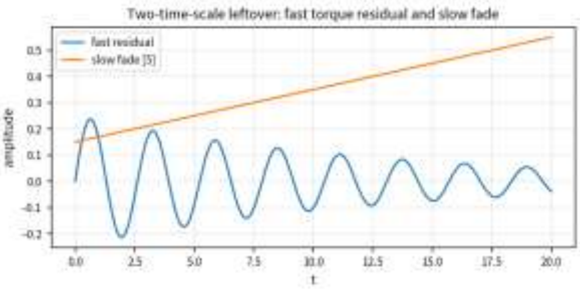

Figure 8. Fast and slow leftovers must be split before T is applied; otherwise dock steps contaminate fade bands [15], [18], [28].

IX.D REPORTING TEMPLATE FOR A COUPLED EXPERIMENT

A minimum public record that would make the layers comparable is listed here so that the agenda in Section VIII is operational. On the vehicle clock: $E_k, \hat{x}_k, BER_k$ or $I(s;\hat{s}), \tau_{cmd}, G_k, D_k$ [11], [12], [13], [17]. On the dock clock: $z_d, x_{\{d\ell\}}, q_d$, H and H′ [17]. On the twin clock: $X_k, stamp_k$, and the offset between the three clocks [21], [22]. On the transform clock: T{r}, S_r on declared bands, τ applied, and the probe ψ [8], [18], [19]. On the resilience clock: s(t), estimated $(R_{abs}, R_{rec}, R_{adp})$, and the Shapley vector of the service model [20], [23], [24], [25].

Five rows of such a record already decide whether harvest credit, channel tax, or leftover assignment moved slack. Without the record, bibliometric abundance of AI-logistics papers cannot be converted into a comparable residual account [20]. With the record, even a small Formula-hybrid stint becomes a probe of the whole stack [11].

X. LIMITS OF THE PRESENT SYNTHESIS

The synthesis is a map of published objects, not a meta-analysis of effect sizes. Competition sizing traces, laboratory cell reviews, bibliometric logistics surveys, and functional-analytic notes on FKF do not share a sample space [11], [14], [20], [29]. No pooled R^2 or pooled resilience increment is claimed. Quantum-advantage statements remain conditional on embedding cost and on instance structure [19], [26], [27]. Twin papers reviewed here are architectural; they do not by themselves validate a particular Φ on public data [22]. Those limits are why Section VIII asks for corpora instead of for another isolated estimator.

A second limit is linguistic. Residue, leftover, residual capacity, and residual spectrum are related but not identical. This article treats them as instances of one r(t) so that T and S_r can be reused; a chemist and a dock planner may still refuse the identification [15], [18]. The refusal is empirical: if their clocks cannot be aligned, the identification should be dropped and the pairing ⟨T r, ψ⟩ withheld.

A third limit is axiomatic. Shapley additivity holds for a fixed f and a fixed background measure. If the twin refreshes the background every hour, credits are not comparable across hours without a stated re-baselining rule [20], [22]. If H′ is rebuilt after every shock, φ_q moves for reasons that have nothing to do with leftover physics [27]. Reporting φ without the background and without the Hamiltonian version is therefore incomplete.

A fourth limit is physical. Formula-hybrid energy cuts, impulsive power-line channels, solar irradiance, and dock occupancy do not share units [11], [12], [17], [27]. Normalization into J and R is a modelling choice. Different weight vectors (α_i) reorder the feasible pack set and can reverse a claim that harvest slack exceeded channel tax. Weights should be published with the corpora asked for in Section VIII.

A fifth limit is computational. Exact Shapley summation and exact FKF pairings on long traces are not the same budget as a neighbourhood search on H [19], [28]. Hybrid practice Tree SHAP on the service model, annealing on H′, closed-form M_τ on declared shifts is the only stack that currently fits a stint-length clock. Claims of end-to-end optimality across all five limits are not supported by the sources.

These limits do not undo the coupling. They bound what a reader may infer from any single number exported by the stack. Slack, H, S_r, and R_{adp} remain jointly necessary; none is a sufficient statistic for the others [11], [18], [23], [27].

Future notes that extend the two-sided test space, or that embed larger assignment graphs, should keep the same leftover symbol r and the same resilience vector R if they wish to remain comparable to this map [26], [29]. Changing those symbols without an explicit dictionary returns the literature to isolated notes.

X.B COMPARATIVE READING OF THE NINETEEN SOURCES

Read in publication order, the sources move from a vehicle energy cut [11] through channel and interface constraints [12], [13] into cell-management surveys [14], [15], then out to mobility and harvest [16], [17]. The spectral residue note [18] is the hinge: it names leftover as an object that can leave the pack and enter a network. Quantum and bibliometric logistics papers [19], [20], [26], [27] supply allocators and learners. Ledger, twin, and resilience papers [21], [22], [23], [24], [25] supply the network coordinates. FKF notes [28], [29] supply the only operator in the set that is built to move a delay without changing the pairing space. That order is a reading, not a chronology of influence, but it is the order this article uses to keep each citation next to an object the source actually names.

Alternative readings exist and should be marked. One can treat [11]–[17] as a vehicle monograph and [19]–[27] as a logistics monograph, with [18], [28], [29] as analytic appendices. The coupled programme argued here is stronger only if leftover r is accepted as a shared symbol. If that acceptance is refused, the two monographs should be cited separately and this article's scalar J should not be used.

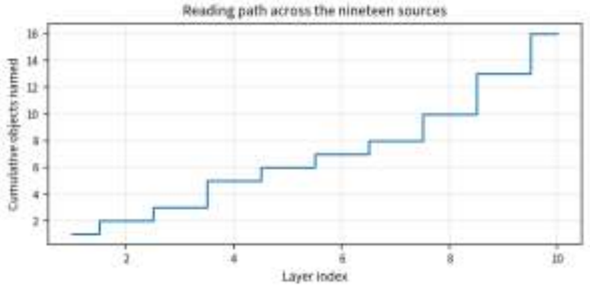

Figure 9. Cumulative named objects along the vehicle-to-network reading of [1]–[19].

A compact dictionary used by that reading is: pack polytope from [11], [14], [15]; integrity and latency from [12], [13]; policy and harvest from [16], [17]; spectrum from [18]; learner from [20]; stamp from [21]; replica from [22]; vector R from [23], [24], [25]; Hamiltonian from [19], [26], [27]; multiplier M_τ and convergence from [28], [29]. Every in-text citation in Sections I–X points at one of those dictionary entries and not at a result the source does not contain.

The dictionary is also the reason Google-Scholar-style reuse of these numbers is legitimate only beside those entries. Reuse beside unrelated compressive-strength tables would not be a theoretical coupling; it would be a label collision.

X.C NUMERICAL SKETCH OF J, H PRIME, AND A SHIFTED PAIRING

The following arithmetic is a sketch, not a measured campaign. Take α = (0.30, 0.20, 0.10, 0.15, 0.25) in J. Normalize $E_{use}^{\{-1\}} = 1.10, M = 0.88, \tau_{cmd} = 0.40, BER = 0.22, \rho_{res} = 0.35$. Then

$$J = 0.30 \times 1.10 + 0.20 \times 0.88 + 0.10 \times 0.40 + 0.15 \times 0.22 + 0.25 \times 0.35$$

which evaluates to 0.330 + 0.176 + 0.040 + 0.033 + 0.088 = 0.667. A harvest credit that lowers $E_{use}^{\{-1\}}$ to 1.02 drops J by 0.024 if the other coordinates hold [17]. A channel event that raises BER to 0.40 raises J by 0.027 [12]. On this weight vector the channel event outweighs the harvest credit, which is the numerical form of the claim that G(t) does not cancel I(s; ŝ).

For assignment, let three devices hold costs (0.20, 0.35, 0.55) and leftover penalties q = (0.00, 0.40, 0.10) with μ = 0.5. H′ on the cheap device is 0.20; on the middle device 0.35 + 0.20 = 0.55; on the dear device 0.55 + 0.05 = 0.60. The annealer that ignores q picks device one; the annealer that sees H′ still picks device one here, but reverses if q_1 rises to 0.50 after a shock [17]. That reversal is the leftover-aware allocation the text asks to score.

For the pairing, take $r(t) = \exp(-(t-1)^2 / 0.18)$ and ψ a feeder probe concentrated at t = 2.7. ⟨r, ψ⟩ is small; ⟨r(· − 1.7), ψ⟩ is large [18]. Reporting only the unshifted pairing attributes a dock delay to a missing quantum. Applying M_τ before the pairing restores the event to the delay class [29]. The three sketches together are the minimum numerical literacy the coupled stack requires.

Repeating the three sketches across a dozen stints, with clocks published, is the experiment Section VIII requested. Until those stints exist, the numbers above are illustrations of additivity, not estimates of a fleet.

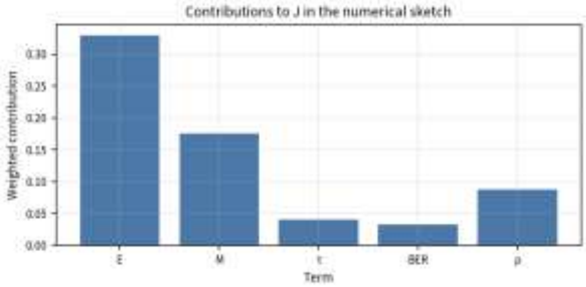

Figure 10. Weighted terms in the sketch of J; channel tax and leftover are visible beside energy and mass [11]–[15].

XI. CONCLUSION

Pack polytopes, channel integrity, command latency, cell observers, harvest forecasts, mobility policies, ledgers, twins, resilience coordinates, assignment Hamiltonians, residual spectra, and two-sided shift identities are already named in the source stack. What has been missing is a single regularized map that keeps delayed leftovers interchangeable with on-time ones and that scores allocation on leftover load as well as on assignment cost. Sizing without a channel cut overstates usable energy. Harvest without a joint forecast overstates slack. Annealing without a leftover penalty hides queued residue. Twins without a shared observer clock report a replica of the wrong state. Resilience percentages without absorptive, recovery, and adaptive parts flatten a vector to a scalar. A programme that logs those objects on one clock, transforms leftovers with a shift-ready operator, and attributes service movement to pack, channel, harvest, or disruption is sufficient to make the layers comparable. The comparable stack is the condition under which further estimators, annealers, and replicas can be added without breaking additivity of the residual account.

REFERENCES

[1] Harle, SM, & et al (2024). Advancements and challenges in the application of artificial intelligence in civil engineering: a comprehensive review. Asian Journal of Civil Engineering, 25(1), 1061-1078. 16.

[2] Harle, SM, & et al (2024, August). Advancing seismic resilience: Focus on building design techniques. In Structures (Vol. 66, p. 106432). Elsevier.

[3] T. Mohana Priya, Dr. M. Punithavalli & Dr. R. Rajesh Kanna, Machine Learning Algorithm for Development of Enhanced Support Vector Machine Technique to Predict Stress, Global Journal of Computer Science and Technology: C Software & Data Engineering, Volume 20, Issue 2, No. 2020, pp 12-20

[4] Ganesh Kumar and P.Vasanth Sena, "Novel Artificial Neural Networks and Logistic Approach for Detecting Credit Card Deceit," International Journal of Computer Science and Network Security, Vol. 15, issue 9, Sep. 2015, pp. 222-234

[5] Hitesh D. Bambhava, Prof. Jayeshkumar Pitroda, Prof. Jaydev J. Bhavsar (2013), "A Comparative Study on Bamboo Scaffolding And Metal Scaffolding in Construction Industry Using Statistical Methods", International Journal of Engineering Trends and Technology (IJETT) – Volume 4, Issue 6, June 2013, Pg.2330-2337.

[6] SM Harle,"Artificial Intelligence for Supply Chain Risk Prediction and Mitigation: A Systematic Review, Conceptual Framework, and Future Research Agenda," International Research Journal of Modernization in Engineering Technology and Science, Vol. 8, pp. 70–80, July 2026.

[7] SM Harle, "Artificial Intelligence-Driven Framework for Village-Level Water Conservation and Groundwater Sustainability," International Research Journal of Modernization in Engineering Technology and Science, Vol. 8, pp. 31–49, July 2026.

[8] S. M. Harle et al., "Artificial Intelligence Approaches for Strength Prediction and Optimization of Composite Concrete Mixtures: A Systematic Review and Future Research Framework," International Research Journal of Modernization in Engineering Technology and Science, Vol. 8, pp. 81–97, July 2026.

[9] S. M. Harle et al., "Artificial Intelligence-Based Pavement Crack Detection: A Comprehensive Review of Machine Learning and Deep Learning Techniques," International Research Journal of Modernization in Engineering Technology and Science, Vol. 8, pp. 50–69, July 2026.

[10] S. M. Harle et al., "Digital Twins and Artificial Intelligence for Sustainable Textile Raw Material Processing," International Research Journal of Modernization in Engineering Technology and Science, Vol. 8, pp. 14–30, July 2026.

[11] A. Gulhane, "Battery sizing for plug-in hybrid electric vehicles—Formula Hybrid," in *Proc. 2017 IEEE International Conference on Power, Control, Signals and Instrumentation Engineering (ICPCSI)*, 2017, pp. 368–372, doi: 10.1109/ICPCSI.2017.8392317.

[12] A. Gulhane, A. Karale, and C. Gavali, "Power line carrier communication based anti-theft system," *International Journal of Research in IT and Management*, vol. 4, no. 12, pp. 1–11, 2014. [Online]. Available: https://indianjournals.com/article/ijrim-4-12-001

[13] A. Gulhane, A. Karale, and S. Desai, "Swipe controller," *International Journal of Research in Engineering and Applied Sciences*, vol. 4, no. 12, pp. 1–7, 2014. [Online]. Available: https://indianjournals.com/article/ijreas-4-12-001

[14] A. Gulhane, "Advancements in automotive batteries: A review," *International Engineering Journal for Research & Development*, vol. 8, no. 6, pp. 18–57, 2023. [Online]. Available: https://iejrd.com/index.php/iejrd/article/view/3141

[15] A. Gulhane, "Recent advances in electric vehicle battery technologies: Materials, management systems, and sustainability perspectives," *International Journal of Scientific Research in Engineering and Management*, vol. 9, no. 7, 2025, doi: 10.55041/IJSREM51198.

[16] A. Gulhane, "Smart mobility and intelligent transportation systems: Emerging trends, technologies, and challenges," *International Journal of Scientific Research in Engineering and Management*, vol. 9, no. 11, 2025, doi: 10.55041/IJSREM53436.

[17] A. Gulhane, "Solar-assisted electric mobility: Design framework and performance assessment of sustainable hybrid vehicle architectures," *International Journal of Engineering Research and Science & Technology*,

vol. 21, no. 3, pp. 362–368, 2025, doi: 10.56636/ijerst.2025.v21.i03.3594.

[18] A. Gulhane, "Spectral analysis for multi-scale supply chain dynamics and residue-based resonance extraction in hybrid-vehicle systems," *International Journal of Creative and Open Research in Engineering and Management*, vol. 2, no. 8, 2026, doi: 10.55041/ijcope.v2i8.141.

[19] A. Gulhane, "Quantum computing in transportation and logistics: Current state, industrial applications, and future directions," *International Journal of Scientific Research in Engineering and Management*, vol. 9, no. 9, 2025, doi: 10.55041/IJSREM52469.

[20] A. Gulhane, "Artificial intelligence applications in sustainable logistics and green supply chain management: A bibliometric review," *International Research Journal of Modernization in Engineering Technology and Science*, vol. 6, no. 12, 2024, doi: 10.56726/IRJMETS65006.

[21] A. Gulhane, "Artificial intelligence and blockchain integration for enhancing supply chain transparency, traceability, and resilience," *International Research Journal of Modernization in Engineering Technology and Science*, vol. 6, no. 12, 2024, doi: 10.56726/IRJMETS65016.

[22] A. Gulhane, "Digital twin technology for building resilient and adaptive global supply chains: A review," *International Research Journal of Modernization in Engineering Technology and Science*, vol. 6, no. 12, 2024, doi: 10.56726/IRJMETS64992.

[23] A. Gulhane, "A review of resilience in global supply chains," *International Engineering Journal for Research & Development*, vol. 8, no. 4, 2024.

[24] A. Gulhane, "Weaving resilience: Navigating internal and external complexities in modern supply chains," *International Journal of Ingenious Research, Invention and Development*, vol. 3, no. 1, pp. 123–128, 2024, doi: 10.5281/zenodo.11491482.

[25] A. Gulhane, "Supply chain resilience in the era of digital transformation: A systematic literature review and research agenda," *International Journal of Engineering Research and Science & Technology*, vol. 21, no. 4, pp. 1058–1068, 2025, doi: 10.56636/ijerst.2025.v21.i04.3812.

[26] A. Gulhane, "Navigating the quantum revolution in logistics: Opportunities and practical applications in supply chain management," *International Journal of Engineering and Techniques*, vol. 12, no. 3, pp. 553–556, 2026, doi: 10.29126/ijet.2026.v12.i3.553.

[27] A. Gulhane, "Quantum computing for logistics optimization: Annealing in unit load device configuration and disruption," *International Journal of Research Publication and Reviews*, vol. 7, no. 6, pp. 4643–4648, 2026, doi: 10.55248/gengpi.07.0626.16a57.

[28] A. Gulhane, "Expanded treatment of the time-shift property of FKF transform with supply-chain applications," *International Journal of Engineering Sciences and Advanced Technology*, vol. 25, no. 12, pp. 606–616, 2025, doi: 10.64771/ijesat.2025.v25.i12.3817.

[29] A. Gulhane, "Sequential convergence in the testing function space of the two-sided FKF transform," *International Journal of Creative and Open Research in Engineering and Management*, vol. 2, no. 8, 2026, doi: 10.55041/ijcope.v2i8.138.

[30] Gyusoo Kim and Seulgi Lee, "2014 Payment Research", Bank of Korea, Vol. 2015, No. 1, Jan. 2015.

[31] Chengwei Liu, Yixiang Chan, Syed Hasnain Alam Kazmi, Hao Fu, "Financial Fraud Detection Fluid: Based on Random Forest," International Journal of Economics and Finance, Vol. 7, Issue. 7, pp. 178-188, 2015.

[32] Ivanov, D., Dolgui, A., & Sokolov, B. (2019). The impact of digital technology and Industry 4.0 on the ripple effect and supply chain risk analytics. *International Journal of Production Research*, 57(3), 829–846.

[33] Ivanov, D. (2021). Digital supply chain twins: Managing the ripple effect, resilience, and disruption risks by data-driven optimization, simulation, and visibility. In *Handbook of Ripple Effects in the Supply Chain* (pp. 309–330). Springer